

# Topological Effects of Spike Timing-Dependent Plasticity

James Kozloski and Guillermo A. Cecchi

*Computational Biology Center, IBM Research Division,*

*IBM T.J. Watson Research Center, Yorktown Heights, NY 10598*

(Dated: April 26, 2019)

## Abstract

We show that the local Spike Timing-Dependent Plasticity (STDP) rule has the effect of reducing the trans-synaptic weights of closed loops of any length within a simulated network of neurons. We further prove analytically that anti-loop learning and STDP are equivalent for the case of a linear network. Thus a notable local synaptic learning rule yields structures dominated by feed-forward connections at their largest scale. Given its widespread occurrence in the brain, we propose that STDP must be involved in eliminating long range synaptic loops among individual neurons across all brain scales, up to, and including, the scale of global brain network topology.

## I. INTRODUCTION

Connections between individual neurons in the brain arise first from the spatial distribution of axons and dendrites within neural tissue [? ][? ]. No consistent framework yet explains how the brain self-organizes to yield function at the global scale. Comprising densely connected networks embedded in neuroanatomical areas and structures joined by bidirectional connections, global brain network topology is not yet fully specified at the level of micro-circuitry [1]. One proposal for a rule governing this level of organization, the “no strong loops hypothesis,” considered only developmentally determined area to area connectivity patterns to implement its specific neuron to neuron network topological constraint [? ]. While local synaptic modification rules are known to shape patterns of connectivity in local neural tissue and local micro-circuit topology, our understanding of global brain network topology still derives largely from this patterned area to area connectivity determined during development. Furthermore, measuring simultaneously the relative strengths of specific micro-circuit connections remains technically challenging, and virtually impossible for even medium sized (50 – 100 neurons, 0.1 – 0.5 mm) micro-circuits. For these reasons, it is not yet known how micro-circuit topology and the computation it supports emerges in the brain beyond the local scale.

We wondered whether a synaptic modification rule commonly observed in brain structures, STDP [? ], could be analyzed to yield an understanding of what global brain network topology it predicts at the micro-circuit level. STDP is a departure from traditional Hebbian models of learning, which state that neurons that fire action potentials together will have their interconnections strengthened. Instead, STDP takes into account the particular temporal order of pre- and post-synaptic neuron firing. Thus, the rule modifies synapses anti-symmetrically, depending on whether the pre- or post-synaptic neuron fires first (Fig.1). What is the influence of this anti-symmetry on global brain network topology?

Consider first if a pre-synaptic “trigger” neuron causes a post-synaptic, first-order “follower” neuron to fire. If this follower makes a direct feedback connection onto the trigger, the feedback connection will be weakened, since the spike generated by the follower will arrive at the follower-trigger synapse immediately after the trigger neuron’s backward propagating action potential. If the backward propagating action potential is delayed by the trigger’s dendritic arbor, this effect may be mitigated or even reversed, but for all other situations in

which axonal propagation time is greater than dendritic propagation time to the synapse, the effect holds. Furthermore, and most importantly, it holds for *all* polysynaptic loops connecting triggers and followers: if some  $n^{\text{th}}$ -order follower's action potential arrives at the original trigger after the trigger has fired, the loop will be broken by spike-timing dependent synaptic weakening. With this intuition, we set out to prove analytically and by means of numerical simulation that network topology, and specifically the density of loops in highly connected networks, is directly and necessarily determined by STDP.

## II. RESULTS

### A. Analytical proof of the equivalence of STDP and anti-loop learning

First, we represent STDP acting on a weight  $w$  associated with the connection between two neurons and their output variables  $x(t)$  to  $y(t)$ , in the adiabatic approximation (i.e. small learning rate), as:

$$\Delta w \propto \int_{-\infty}^{\infty} C(t)S(t)dt \quad (1)$$

where  $C(t) = \int x(t' - t)y(t')$  is the correlator, and  $S(t)$  is the anti-symmetric STDP update function,  $S(t < 0) = \exp(\lambda t)$ ,  $S(t > 0) = -\exp(-\lambda t)$ . Consider this function operating over connections within a linear network driven by uncorrelated Gaussian inputs,  $\vec{\xi}$ , such that  $\dot{\vec{x}}(t) = \mathbf{W}\vec{x}(t) + \vec{\xi}(t)$  [2]. We show (see Appendix A) that the learning rule defined in Eq. 1 results in an update for the network weight matrix of the form  $\Delta \mathbf{W} = \Delta \mathbf{W}(\mathbf{W}, \tau, C_0)$  where  $\tau$  is the time constant of the STDP's exponential,  $C_0$  is the instantaneous correlator, i.e.  $C(0)$ , and  $^\dagger$  stands for the transpose operation. This update rule influences global network topology in a very specific way. To formalize our original intuition analytically, consider a linear network with only excitatory connections, such that the dynamics may be expressed as  $\dot{\vec{x}} = \mathbf{W}\vec{x} = (-\mathbf{1} + \mathbf{A})\vec{x}$ , where  $A_{ij} \geq 0$  is the network connectivity matrix (comprising the non-diagonal elements of the weight matrix and zeros on the diagonal), and  $-\mathbf{1}$  represents a self-decay term. Next, we introduce a “loopiness” measure that estimates the density of loops of all sizes throughout the network,  $\mathcal{E}_l = \sum_{n=1}^{\infty} \frac{1}{n} \text{tr}(\mathbf{A}^\dagger)^n$ . The function  $\text{tr}$  stands for the trace operation; this operation, when acting on the  $n$ -exponentiation of the adjacency matrix (comprising ones and zeros), counts the total number of closed paths of length exactly equal to  $n$ , i.e.  $n$ -loops [3]. When applied to the network connectivity matrix

$\mathbf{A}$ , the operation counts loops weighted by the synaptic strength of the connections. It is possible, however, to reduce this measure without actually eliminating topological loops, by simply reducing the weights of all connections. A proper *topological* loopiness measure must therefore include a penalty to the weights’ vanishing; we choose  $-\frac{1}{2}\text{tr}\mathbf{A}^\dagger\mathbf{A}$ , which generalizes to weighted graphs a measure that counts the number of links for a binary graph. The total loopiness is then defined as:

$$\mathcal{E} = \sum_{n=1}^{\infty} \frac{\tau^n}{n} \text{tr}(\mathbf{A}^\dagger)^n - \frac{1}{2} \text{tr}\mathbf{A}^\dagger\mathbf{A} \quad (2)$$

We show (see Appendix B) that the change in this energy as a function of the evolution of the network,  $\Delta\mathcal{E} \sim \text{tr} \partial\mathcal{E}_{\mathbf{W}}\Delta\mathbf{W}^\dagger$ , is strictly semi-negative, and therefore the evolution of the network under STDP results in a decrease of the “loopiness”. Having proven their equivalence, we therefore use the term STDP and “anti-loop learning” interchangeably throughout.

## B. Anti-loop learning in a network of simulated neurons

What are the effects of this form of plasticity on network topology in nonlinear networks, such as those found in neural microcircuits? Because our proof of the equivalence of STDP and anti-loop learning applies only to linear networks or nonlinear networks that may be linearized, we aimed to show, using simulation, that the same principle extends to a biologically relevant, nonlinear regime. We replicated the simulation of Song and Abbott [? ], extending it in three ways (see Section IV). First, we created a network of 100 neurons, each receiving excitatory synapses from all other 99 “intra-network” input sources and from 500 randomly spiking “extra-network” input sources selected at random from 2,500 homogenous Poisson processes. All excitatory synapses underwent STDP. Second, we provided 250 inhibitory synapses to each neuron, sampled from 1,250 spiking sources; the inhibitory inputs modeled fast local inhibition to the network using inhomogenous Poisson processes with rates modulated by the instantaneous aggregate firing rate of the network. Third, we explored four different forms of STDP update [? ] and observed robust anti-loop learning for each; the results presented here used the STDP update rule of Gütig et al. [? ].

We initialized our network with maximum extra-network weights, and intra-network weights at half maximum. This caused the network to spike vigorously when extra-network inputs became active, but spike rates were limited by the fast local-inhibition. After 10

seconds of simulated network activity, STDP had a profound effect on loopiness as defined in Eq. 2 (Fig.2A). After 100 seconds of simulated activity, we counted the number of closed loops of varying length using  $\text{tr}([\mathbf{A}]^\dagger)^n$ , where  $[\mathbf{A}]$  was constructed by applying a sliding threshold to the network connectivity matrix (Fig.2B). We compared this quantity to the same, measured for a network constructed by randomly assigning weights from the learned weight distribution to synapses in the network. These results are representative of all loop lengths measured ( $n \leq 100$ ) and show that as the weight threshold grows, the number of closed loops in the STDP-learned network grows increasingly smaller than in the randomized network.

### C. The effect of synaptic delays on anti-loop learning

We wondered what effect synaptic delays would have on this result, since we expected follower feedback spikes to cause less anti-loop learning as they fell further from the zero time difference maxima in the STDP update function. We also wondered if the decrease in the number of loops compared to a randomized network also applied to unique loops, in which no neuron is traversed more than once. We therefore sampled the number of unique loops through networks simulated with synaptic delays from 0.01 to 4.0 milliseconds. We constructed one million random paths of length  $n-1$  for each loop length  $2 \leq n \leq 25$ , and for the learned and randomized networks. We searched for each path across all networks studied, and if the path and the  $n^{\text{th}}$  link completing the loop existed in the network, we counted it for that network. The result is similar to that for closed loops, and, as expected, longer synaptic delays resulted in an exponential decrease in the number of loops as a function of loop length that deviated less from the same function for random networks, indicating weaker anti-loop learning (Fig.2C).

### D. Network in-hubs, out-hubs, and anti-loop learning

Next, we asked if other topological measures of the STDP-learned networks may be correlated with our observation, since many different topological properties might coincide with or support this effect. For example, one means to create networks poor in loops is to ensure that nodes in the network are either “out-hubs” or “in-hubs,” but not both. An out-

hub in a network of neurons has many strong postsynaptic connections but few presynaptic connections, and an in-hub has many strong presynaptic connections but few postsynaptic connections. We applied a sliding threshold to the network connectivity matrix learned by STDP, and examined the manifold of in-degree versus out-degree for each neuron in our network. This showed a clear inverse relationship between in- and out-degrees that varied in form with weight threshold (Fig.3A). In contrast, by examining the in-degree from extra-network inputs, we found a positive correlation (Fig.3B), indicating that out-hubs were more likely to be in-hubs within the larger extra-network topology, and that in-hubs in our network were more likely to receive only the weakest extra-network inputs.

### **E. Reverse STDP restored loops after anti-loop learning**

Beyond these standard topological analyses, we also examined biological properties of the network. We measured total synaptic input as a function of total synaptic output for all neurons in the STDP-learned network. In the same experiment, we asked if reversing the polarity of the STDP function might undo the effects of anti-loop learning, since under this “reverse” condition, follower spikes would cause strengthening of closed-loop feedback connections. This reversal of polarity is biologically relevant, since it has been observed at the synaptic interface between major brain structures [? ], and that cholinergic and adrenergic neuromodulation can control it [? ]. We found an inverse relationship between total synaptic input and output following 15 seconds of forward STDP. This relationship could be reversed by 85 additional seconds of reverse STDP, in contrast to 85 additional seconds of forward STDP, which strengthened it (Fig.4A). We also found that the total extra-network synaptic input varied positively with total intra-network synaptic output, and that this effect was also reversed by reverse STDP (Fig.4B).

### **F. Dynamical effects of anti-loop learning**

What are the consequences of this form of network plasticity beyond topology? In the case of a linear network, reducing the number of loops implies more stable dynamics. Consider the stability of the unforced system  $\dot{\vec{x}}(t) - \mathbf{W}\vec{x}(t) = 0$ ; assuming the system is stable, the

eigenvalues can be expressed as:

$$-\sum_{i=1}^N \log |\lambda_i| = \sum_{k=1}^{\infty} \frac{1}{k} \text{tr} \mathbf{A}^k \quad (3)$$

which, given that stability requires that all eigenvalues be negative, emphasizes the contribution of loops to system instability: adding loops implies moving the eigenvalues closer to zero. Such a simple observation, however, does not make clear predictions about the effects anti-loop learning on nonlinear neural circuit function. We were surprised to find that raster plots of network spiking activity, when sorted according to certain topological metrics (e.g., the sum of extra-network input weights, the sum of intra-network output weights, in-degrees, out-degree) consistently reveal network events that originate with weak synchronization among out-hubs, followed by strong synchronization among in-hubs (Fig.5A, top). This effect was altered by randomizing the intra-network weights, such that synchronization events became stronger, more frequently global, and more frequent among out-hubs alone (Fig.5A, bottom). Peri-event time histograms reveal this same effect (Fig.5B, left panels), with synchronization arising strongly among in-hubs after weak out-hub activation in the STDP-learned network, and globally in the randomized network. In the STDP-learned network, both in-hubs and out-hubs sustain spike rates ranging from 4 – 9 Hz that are not correlated with in-degree, whereas in the randomized network, spike rates range more broadly (3 – 16 Hz) and are highly correlated with in-degree (Fig.5B, right panels). We examined the summed network peri-event time histograms for the STDP-learned network, and for networks that underwent randomization of their intra-network weights, their extra-network weights, or both (Fig.5C, top). The resulting distributions showed higher kurtosis and more negative skew when intra-network weights were randomized (Fig.5C, bottom), indicating that the effect of anti-loop learning is to generate network events that have greater spread and symmetry in time.

### III. DISCUSSION

Based on our simulations and analytic results, we conclude that STDP produces a network topology that is conspicuously poor in both closed and unique loops, and that it segregates neurons into out- and in-hubs to achieve this. Furthermore, the network that emerges organizes its relationship to random Poisson inputs in an orderly fashion, making out-hubs

the primary target for input, and thus establishing a feed forward relationship between the network and its pool of inputs. In a larger system, we anticipate that network in-hubs would become out-hubs relative to the larger network topology.

Interestingly, the depletion of loops and the separation of nodes into out-hubs and in-hubs has been recently reported in a variety of complex biological systems, including functional networks at the level of spatio-temporal resolution of fMRI, and the neural network of *C. Elegans* [? ], suggesting a general principle of organization and dynamical stability for entire classes of functional networks.

Finally, we observe that network activity propagates smoothly through this feed-forward topology without segregating neurons by average spike-rates. The effect on global brain function of such properties would include stable average firing rates shared among all neurons, regardless of their topological position, and robust signal propagation, similar to “synfire chains” [? ? ]. STDP and its modulation [? ], therefore, represent potent organizing influences on global brain network topology and on global brain dynamics.

#### IV. METHODS

The simulation methods of Song and Abbot [? ] were used to simulate each neuron in our 100 neuron network. Briefly, each neuron model was integrate-and-fire, with membrane potential determined as in [? ], by  $\tau_m \frac{dV}{dt} = V_{rest} - V + g_{exc}(t)(E_{exc} - V) + g_{inh}(t)(E_{inh} - V)$ , with  $\tau_m = 20\text{ms}$ ,  $V_{rest} = -60\text{mV}$ ,  $E_{exc} = 0\text{mV}$ ,  $E_{inh} = -70\text{mV}$ ,  $V_{thresh} = -54\text{mV}$ , and  $V_{reset} = -60\text{mV}$ .

The synaptic conductances  $g_{exc}$  and  $g_{inh}$  were modified by the arrival of a presynaptic spike, as in [? ], such that  $g_{exc}(t) \rightarrow g_{exc}(t) + \bar{g}_a$ , and  $g_{inh}(t) \rightarrow g_{exc}(t) + \bar{g}_{inh}$ . In the absence of a spike, these quantities decay by  $\tau_{exc} \frac{dg_{exc}}{dt} = -g_{exc}$ , and  $\tau_{inh} \frac{dg_{inh}}{dt} = -g_{inh}$ , with  $\tau_{exc} = \tau_{in} = 5.0$ ,  $\bar{g}_{in} = 0.015$ ,  $0 \leq \bar{g}_a \leq \bar{g}_{max}$ , and  $\bar{g}_{max} = 0.01$ . We initialized  $\bar{g}_a$  to different values for intra-network ( $\bar{g}_a = 0.005$ ) and extra-network ( $\bar{g}_a = 0.01$ ) inputs.

For extra-network inputs, excitatory homogenous Poisson spike trains were generated at a rate of 20 Hz. Inhibitory, inhomogenous Poisson spike trains that model fast local inhibition were generated at a rate  $r_{min} \leq r_{inh} \leq r_{max}$ , where  $r_{min} = 5$  Hz, and  $r_{max} = 1000$  Hz. On each time step,  $dt = 0.1$  ms,  $r_{inh}$  is incremented by an amount proportional to the fraction,  $\gamma$ , of network neurons that spiked during that timestep, and decays with a time constant,



$\tau_r$ , such that  $\tau_r \frac{dr_{inh}}{dt} = -[r_{inh} + (r_{max} - r_{min})\gamma]$ . After this update, if  $r_{inh}$  exceeds  $r_{max}$ ,  $r_{inh} \rightarrow r_{max}$ .

For all simulations we report here, the STDP update rule for a synapse from neuron  $j$  to neuron  $i$  was  $\bar{g}_a(i, j) = \bar{g}_a(i, j) + \bar{g}_a(i, j)^\mu M(i)$  for synaptic potentiation, and  $\bar{g}_a(i, j) = \bar{g}_a(i, j) + (\bar{g}_{max} - \bar{g}_a(i, j))^\mu Pa(i, j)$ , for synaptic depression,  $\mu = 0.1$  ( $\bar{g}_a$  is maintained in the interval  $[\bar{g}_{min}, \bar{g}_{max}]$ ). As in [? ],  $M(i)$  and  $P(i, j)$  decay exponentially, such that  $\tau_- \frac{dM}{dt} = -M(i)$  and  $\tau_+ \frac{dPa}{dt} = -Pa$ ,  $\tau_+ = \tau_- = 20$ . Also as in [? ],  $M(i)$  is decremented by  $A_-$  every time a neuron  $i$  generates an action potential,  $A_- = 0.00035$ , and  $Pa(i, j)$  is incremented by  $A_+$  every time a synapse onto neuron  $i$  from neuron  $j$  receives an action potential,  $A_+ = 0.00035$ . This update rule effectively implements the asymmetric function of STDP (see Fig.1).

## APPENDIX A: UPDATE RULE FOR THE WEIGHT MATRIX

The classical definition of Hebbian learning for the weight  $w$  connecting two dynamical variables  $x(t)$  and  $y(t)$  can be written, in its simplest form, as:

$$\Delta W \sim \eta C_{xy} \quad (\text{A1})$$

$$C_{xy} = \int_{-\infty}^{\infty} x(t)y(t)dt \quad (\text{A2})$$

Where  $\eta$  is the learning constant, which for exposition's sake will be set to 1. It is important, however, to keep in mind that in order to write Eqs. A1-A2 we are assuming an adiabatic approximation, i.e. the learning is small enough that the system can be considered to be in steady-state for the purpose of computing the correlation.

A natural extension of Eqs. A1-A2 is to introduce *time*, i.e. to consider delayed as well as instantaneous correlations:

$$\Delta W \sim \int_{-\infty}^{\infty} C_{xy}(t)S(t)dt \quad (\text{A3})$$

$$C_{xy}(t) = \int_{-\infty}^{\infty} x(t' - t)y(t')dt' \quad (\text{A4})$$

It is assumed that the time-dependent weight function vanishes for long delays,  $\lim_{t \rightarrow \pm\infty} S(t) = 0$ ; the classical learning rule is recovered when  $S(t) = \delta(t)$ . If, as experimental results strongly suggest, the weight function displays strict temporal asymmetry, i.e.  $S(t) = -S(-t)$ , then

$$\Delta W \sim \int_{-\infty}^0 C(t)S(t)dt + \int_0^{\infty} C(t)S(t)dt \quad (\text{A5})$$

$$\Delta W \sim \int_0^{\infty} [C(t) - C(-t)]S(t)dt \quad (\text{A6})$$

A linear system driven by uncorrelated input can be described as:

$$\dot{x}(t) = Wx(t) + \xi(t) \quad (\text{A7})$$

where each unit is independently subject to Gaussian white noise  $\xi(t)$ , a vector whose components satisfy  $\langle \xi_i(t)\xi_j(s) \rangle = \sigma^2 \delta_{ij} \delta(t - s)$  (for simplicity, we drop henceforth boldface for matrices; it should be clear from the context when 1 refers to the scale or the identity matrix). The lagged correlator is related to the zero-lagged correlator by [? ]:

$$C(t) = \begin{cases} e^{W|t|}C_0 & t < 0 \\ C_0e^{W^\dagger t} & t > 0 \end{cases} \quad (\text{A8})$$

Hence the expression for the learning update is:

$$\Delta W \sim \int_0^\infty [C_0e^{W^\dagger t} - e^{Wt}C_0]S(t)dt \quad (\text{A9})$$

The temporal behavior of the weight function has been approximated by a piece-wise exponential form:

$$S(t) = \begin{cases} +e^{t/\tau} & t < 0 \\ 0 & t = 0 \\ -e^{-t/\tau} & t > 0 \end{cases} \quad (\text{A10})$$

where  $\tau$  is STDP's time-constant, i.e. it expresses the window over which the plastic changes due to temporal coincidence are significant. Assuming that the network connections are only excitatory, and expressing without further loss of generality  $W = -1 + A$ , we derive the synaptic weight update as:

$$\Delta A \sim [1 - \mu A]^{-1}C_0 - C_0[1 - \mu A^\dagger]^{-1} \quad (\text{A11})$$

where  $\mu = \tau/(1 + \tau)$ . From this expression we can see that the weight update is anti-symmetric, and that a perfectly symmetric system would not be modified. Of course, any small initial asymmetry will eventually be blown up. We can also see that STDP's time constant introduces the proportionality factor  $\mu$ , which can be absorbed by a renormalization of  $A$ ; we will assume therefore  $\mu = 1$  for the remaining of the exposition. Consistently, the limiting behavior of Eq. A11 implies  $\Delta A(\tau \rightarrow 0) = 0$ .

## APPENDIX B: MINIMIZATION OF LOOPS AND DYNAMICS

Now we can estimate the effect of the synaptic time-dependent plasticity expressed by Eq. A11 on the topology of the network. For this, we will postulate a penalty or energy function for what we will call “loopiness” of the network. A measure of the density of loops in the network can be obtained by summing the trace of the exponentiation of the network connectivity matrix,  $\sum_k \text{tr}(A^k)$ . This loop density can be simply minimized by making the

connections vanish, so we need to introduce a regularization penalty to avoid this effect; an obvious measure of the strength of the connections in a network is  $\text{tr}AA^\dagger$ , which in a binary graph would be equivalent to the total number of links. We postulate then the following “loopiness” energy:

$$\mathcal{E} = \sum_k \frac{1}{k} \text{tr}(A^k) - \frac{1}{2} \text{tr}AA^\dagger \quad (\text{B1})$$

The change in this energy upon small changes  $\Delta A$  is expressed as  $\Delta\mathcal{E} \sim \text{tr}(\partial_A \mathcal{E} \Delta A^\dagger)$ ; it can be easily verified that  $\partial_A \mathcal{E} = (1 - A^\dagger)^{-1} - A$ , and therefore:

$$\begin{aligned} \Delta\mathcal{E} &\sim -\text{tr}K_1 - \text{tr}K_2 \\ K_1 &= (1 - A^\dagger)^{-1} [(1 - A)^{-1}C_0 - C_0(1 - A^\dagger)^{-1}] \\ K_2 &= A [C_0(1 - A^\dagger)^{-1} - (1 - A)^{-1}C_0] \end{aligned} \quad (\text{B2})$$

We will demonstrate in what follows that the traces of  $K_1$  and  $K_2$  are strictly semi-positive under the synaptic changes elicited by STDP (i.e. Eq. A11), and therefore the loopiness energy can only decrease over time. Let us consider the first term, which can be rewritten as:

$$\text{tr} \{ (1 - A^\dagger)^{-1} (1 - A)^{-1} C_0 - (1 - A^\dagger)^{-2} C_0 \} \quad (\text{B3})$$

which is of the form

$$\text{tr} QQ^\dagger P - \text{tr} Q^2 P$$

For any matrix  $Q$  and any posdef matrix  $P$ ,  $\text{tr} QP = \text{tr} QU^\dagger \Lambda U = \text{tr} UQU^\dagger \Lambda = \text{tr} \hat{Q}\Lambda$ . Given that  $P$  is posdef,  $\text{tr} QP = \sum_i \lambda_i \hat{Q}_{ii} \geq \lambda_{\min} \hat{Q}_{ii}$ , and then

$$\text{tr} QP \geq \lambda_{\min} \text{tr} Q \quad (\text{B4})$$

On the other hand, for any  $Q$ ,

$$\text{tr} (Q^\dagger - Q)(Q^\dagger - Q)^\dagger \geq 0$$

which upon expanding leads to

$$\text{tr} (QQ^\dagger - Q^2) \geq 0 \quad (\text{B5})$$

and implies together with Eq. B4 the positivity of the term in Eq. B3. The second term in Eq. B2 can also be rewritten as

$$\text{tr} A^\dagger (1 - A)^{-1} C_0 - \text{tr} A (1 - A)^{-1} C_0$$

which, for the same reason presented above, can be reduced to

$$\text{tr} (A^\dagger - A)(1 - A)^{-1}$$

Replacing  $A(1 - A)^{-1}$  by  $(1 - A)^{-1} - 1$ , the term can be transformed to

$$\text{tr} (1) - \text{tr} (1 - A^\dagger)(1 - A)^{-1} = N - \text{tr} (1 - A^\dagger)(1 - A) \quad (\text{B6})$$

We will show next that Eq. B6 is semi-positive. Let us call

$$K_3 = (1 - A^\dagger)(1 - A)^{-1} \quad (\text{B7})$$

It is trivial to see that  $\det(K_3) = 1$ . It is less obvious to see that its eigenvalues  $\lambda_i(K_3)$  satisfy  $|\lambda_i| < 1$ :

$$(1 - A^\dagger)(1 - A)^{-1}v = \lambda v \quad (\text{B8})$$

$$(1 - A)^{-1}v = \lambda(1 - A^\dagger)^{-1}v \quad (\text{B9})$$

$$v^\dagger(1 - A^\dagger)^{-1} = \lambda^* v^\dagger(1 - A)^{-1} \quad (\text{B10})$$

$$v^\dagger(1 - A^\dagger)^{-1}v = \lambda^* v^\dagger(1 - A)^{-1}v \quad (\text{B11})$$

Combining B9 and B11, we obtain

$$v^\dagger(1 - A^\dagger)^{-1}v = |\lambda|^2 v^\dagger(1 - A)^{-1}v \quad (\text{B12})$$

Therefore  $|\lambda|^2 = 1$ , unless  $v^\dagger(1 - A^\dagger)^{-1}$  or  $(1 - A^\dagger)^{-1}v$  are zero, which is not the case as we will show next. Assuming that the system is already stable, it follows that the eigenvalues of  $A$  are constrained,  $\lambda_{\max}(A) < 1$ , which allows the expansion  $Q = (1 - A^\dagger)^{-1} = \sum_{n=0} A^{\dagger n}$ . Let us assume  $Qv = 0$ , and write  $v = \mu + \rho$ , where  $\mu$  and  $\rho$  are in the null and perpendicular spaces of  $A^\dagger$ ,  $N$  and  $P$  respectively. We get then  $Q(\mu + \rho) = \mu + Q\rho$ , which implies  $\mu = 0$  and  $Q\rho = \sum_{n=0} A^{\dagger n}\rho = 0$ . Expanding in the basis of  $P$ ,  $Q\rho = \sum_{n=0} A^{\dagger n} \sum_i (\rho \cdot \hat{e}_i) \hat{e}_i$ . Calling  $\beta_i$  the eigenvalues of  $A^\dagger$ , it follows that  $\forall i \quad \sum_{k=0} \beta_i^k (\rho \cdot \hat{e}_i) = (\rho \cdot \hat{e}_i) / (1 - \beta_i) = 0$ , which implies  $\rho = 0$ , and in turn  $v = 0$ . But this is inconsistent with  $v$  being an eigenvalue of  $K_3$ , and therefore  $Qv \neq 0$ ; a similar argument leads to  $v^\dagger Q \neq 0$ .

Finally, the constraint  $|\lambda_i|^2 \leq 1$  implies  $\text{tr} K_3 \leq N$ , which ensures the semi-positivity of Eq. B6 and in consequence that of the expression  $K_2$  in Eq. B2 and the overall semi-negativity of the change in loopiness.

We have assumed throughout that the system is in a regime of dynamical stability, and presented a case for the stabilizing effect of STDP by linking loops and eigenvalues in Eq. 3. It follows that loopiness minimization (Eq. 2) is equivalent to maximization of stability (as defined by the l.h.s. of Eq. 3), constrained by the total matrix weight. We can further understand this by explicitly expanding to first order the update equation A11 to see the effect on  $\mathcal{U} = -\sum_i \log |\lambda_i|$ . For this we need to solve first for  $C_0$ , which we can approximate assuming the system is driven by homogeneous gaussian noise; in this case, the Lyapunov equation relating the noise, the correlation and the weight matrix, [? ? ]:

$$C_0 W + W^\dagger C_0 = -Q Q^\dagger \quad (\text{B13})$$

(where  $Q Q^\dagger$  is the generalized temperature), can be expanded as

$$C_0 = \sum_{n=0}^{\infty} \frac{1}{2^n} \sum_{k=0}^n \binom{n}{k} A^{\dagger k} Q Q^\dagger A^{n-k} \quad (\text{B14})$$

To first approximation, assuming  $Q Q^\dagger = 1$ ,  $C_0 \simeq 1 + \frac{1}{2}(A + A^\dagger)$ , leading to  $\Delta A \sim A - A^\dagger$ . Through Eq. 3 we obtain  $\delta \mathcal{U} \simeq \frac{1}{2} \text{tr}(A \delta A + \delta A A)$ , and in turn  $\delta \mathcal{U} \simeq (\text{tr} A^2 - \text{tr} A A^\dagger) \leq 0$ , making the system more stable.

## APPENDIX C: COMMENTS

A previous version of the manuscript included a penalization term for loopiness in the form of  $\text{tr} \log A$ ; the term presented in the current version,  $\text{tr} A A^\dagger$  is much more intuitive. The current version therefore includes a different demonstration for the non-negativity of the changes in loopiness as a function of evolution under STDP.

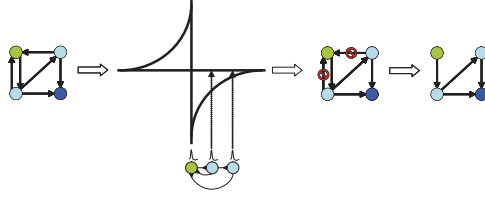


FIG. 1: Schematic of the topological effect of STDP. Feedback connections from “follower” neurons (blue) to the “trigger” neuron (green) create loops. These connections are selectively penalized by the STDP learning rule when spikes propagate through the loopy network (left), resulting in a completely feed forward network (right).

- 
- [1] We use micro-circuitry to refer to neural circuitry observed at the level of neurons and synapses and not necessarily in reference to a restricted spatial extent of these neurons (e.g., a “column”). For this reason, we view every brain connection as part of some micro-circuit topology.
- [2] Let  $\vec{\xi}(t)\vec{\xi}^\dagger(t') = \sigma^2\delta(t - t')\mathbf{1}$
- [3] Note that paths that traverse the same network node more than once are also counted.



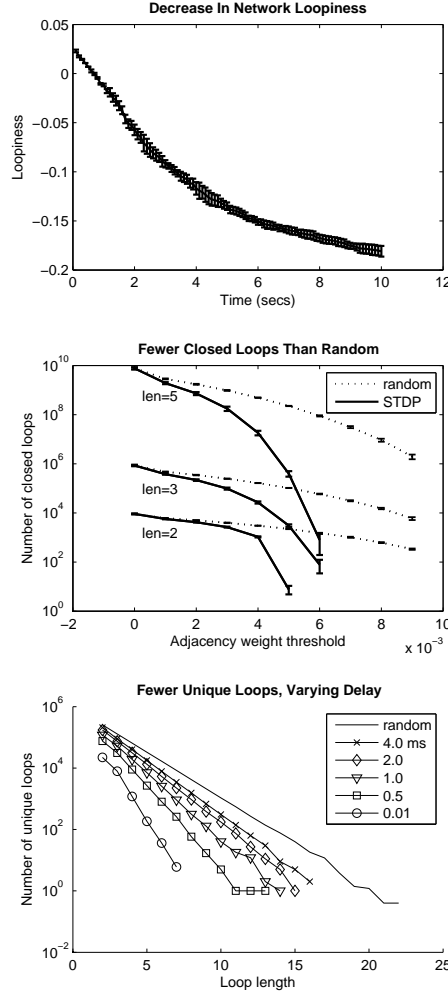


FIG. 2: Global topological effects of STDP. A) A monotonic decrease in the loopiness measure (see text) over time is observed in a simulated network of 100 neurons undergoing STDP. Shown here and in B) is the average of 9 separate simulations; error bars are standard deviation. B) Number of closed loops of length 5, 3, and 2, decreases as a function of weight threshold for network connections. Dotted lines show counts for randomized networks with same number of total connections. C) Number of unique loops sampled for the same network as a function of loop length, with varying synaptic delays. Greater synaptic delays decreases the topological effect of STDP.

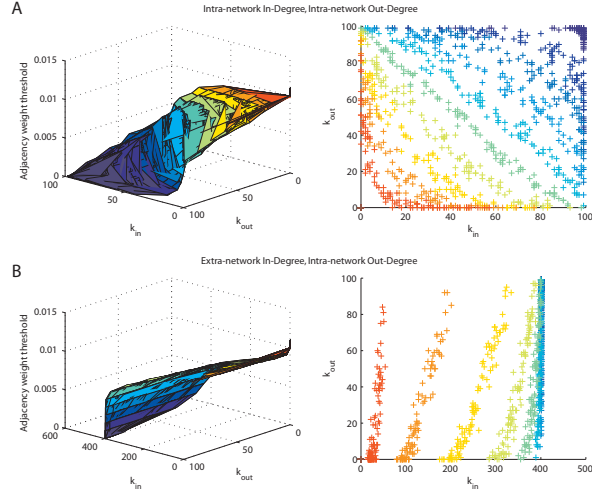


FIG. 3: Local topological effects of STDP. A) Inverse relationship of in-degree versus out-degree of intra-network connections for each neuron in a network after STDP across multiple weight thresholds for network connections. Colors in left and right panels correspond to the same weight threshold. B) Correlated extra-network in-degree and intra-network out-degree indicate an opposite effect of STDP on extra-network inputs.

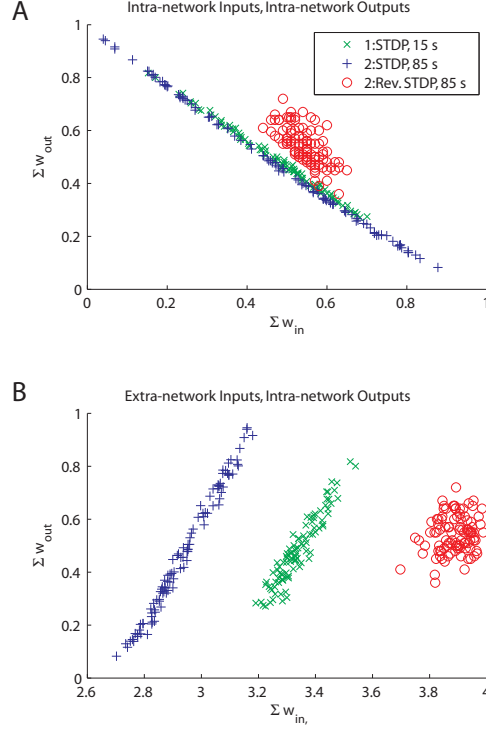


FIG. 4: Effect of reverse-STDP. A) Total synaptic input versus output for intra-network connections. Green and blue markers correspond to the network after 15 then an additional 85 seconds of STDP. Red markers show the result of applying instead reverse STDP (in which the sign of synaptic change as a function of spike timing is reversed) for the additional 85 seconds. The topological effect of STDP is eliminated by reverse STDP. B) Total synaptic extra-network input versus total synaptic intra-network output, plotted as in A.

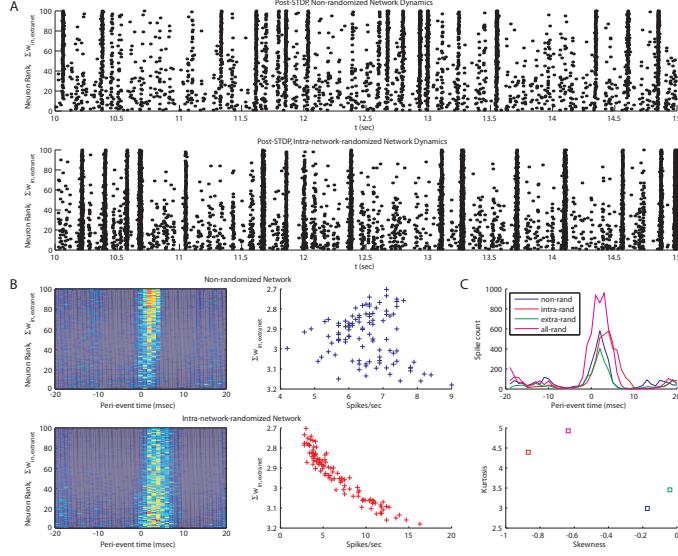


FIG. 5: Dynamical effects of STDP. A) Raster plot of the spiking activity for a network after STDP (top), and for a surrogate network where intra-network weights were reassigned randomly to network connections, thus destroying STDP-learned topology (bottom). Each point corresponds to a spike for each neuron, sorted according to the sum of extra-network input weights. B) Peri-event time histograms for each neuron in the STDP network (top left) and its surrogate (bottom left). Histograms show different network propagation properties. Spike counts and extra-network weights for the same networks do not covary in the STDP-learned topology (top right), but are highly correlated for the surrogate (bottom right). C) Peri-stimulus time histograms summed across all neurons for the STDP network (blue) and three surrogates, in which the intra-network (red), extra-network (green) and all (magenta) network connections were randomized (top). Skewness versus kurtosis of these histograms (bottom) indicates the network distribution of spikes is spread more symmetrically for the STDP-learned topology.